

BY Draconis Stars in Two Galactic Clusters: Exploring the Rotation and Cyclical Variability of the Brighter Members

BRINCAT M STEPHEN^{1,5}; GALDIES CHARLES^{2,5}; GRECH WINSTON³; MIFSUD MARTIN^{4,5}; AND GONZALEZ CARBALLO JUAN-LUIS^{5,6}

- 1) Flarestar Observatory (MPC 171), San Gwann, SGN 3160, Malta, stephenbrincat@gmail.com;
- 2) Institute of Earth Systems, University of Malta, charles.galdies@um.edu.mt;
- 3) Antares Observatory, 76/3, Kent Street, Fgura FGR 1555, Malta,
- 4) Manikata Observatory, Manikata, Malta,
- 5) American Association of Variable Star Observers
- 6) Cerro del Viento Observatory (MPC 184), Badajoz, Spain,

Abstract: This study examines the rotational and cyclic variability of 79 BY Draconis stars in the M45 (Pleiades) and Alpha Persei clusters, refining their rotation and activity cycle periods through Lomb-Scargle periodogram analysis. Photometric data from ASAS-SN, supplemented by observations from multiple observatories, reveal significant differences in period distributions between the clusters, highlighting the influence of stellar age on rotational and magnetic activity cycles. Key findings include a moderate positive correlation between cyclic amplitude (AMP-C) and cyclic period (PCYC), suggesting that stronger magnetic fields require longer timescales for full activity cycles. A strong correlation between rotational amplitude (AMP-R) and cyclic amplitude (AMP-C) supports the link between short-term rotational modulation and long-term stellar magnetic cycles. However, the weak correlation between rotation period (PROT) and cyclic period (PCYC) indicates that additional factors beyond rotation influence cyclic variability. These results contribute an updated dataset of rotational and cyclic periods for BY Draconis stars, reinforcing the importance of long-term monitoring to better understand stellar magnetic evolution and dynamo-driven activity cycles.

1 Introduction

BY Draconis stars are a fascinating class of variable stars. They are main-sequence stars belonging to the FGKM-type stars (Chahal et al., 2022) of which a significant proportion exhibit binarity (Bopp and Fekel, 1977). BY Draconis or BY Dra stars are characterized by periodic brightness variations due to dark spots on their surfaces arising from their magnetic field, which is modulated by their rotation.

By monitoring variations in brightness, color, or spectral features, the rotation period of BY Draconis stars can be measured. Using data from the Zwicky Transient Facility (ZTF) as a baseline and considering factors such as stellar mass, age, and environment, these periods can range from as short as 0.15 days to about 61 days, as reported by Chahal (2022). However, other researchers, such as Watson (2006) and Sanghi et al. (2021), have reported different rotation periods up to 120 days, based on the specific parameters of their studies.

Beyond their rotation period, BY Draconis stars exhibit a cyclic period, marking the time span of a complete magnetic activity cycle. This cyclic period can be determined by observing the star's long-term variations in brightness, color, spectrum, or radio emissions.

The duration of this cycle is quite variable, extending from a few years to multiple decades. Factors such as the star's mass, age, and the surrounding environment play a significant role in influencing the length of this cycle.

The rotation period and the cyclic period of BY Draconis stars are important to study in relation to their magnetic activity and stellar evolution. Magnetic activity is the manifestation of various phenomena on the surface and in the atmosphere of a star, such as spots, flares, prominences, and coronal mass ejections. The interaction between a star's magnetic field and its plasma drives these phenomena and ultimately their evolution (Chahal, 2022).

In this paper, we present our study of the rotation period and the cyclic period of a sample of BY Draconis stars extracted from two galactic clusters namely, M45 (Pleiades) and the Alpha Persei (Melotte 20) in order to update the rotational period of known BY Dra stars and derive the period of stars with unknown period. Another objective of this study was to conduct an analysis to search for correlations between different parameters of these stars.

To achieve these goals, we have embraced a Pro-Am collaborative approach where we merged photometric data from professional sources, such as ASAS-SN, with observations contributed by amateur astronomy observatories, and in so doing is contributes to a uniquely comprehensive and complementary dataset. This synergy not only enables the validation and cross-checking of our findings, increasing the reliability of results, but it also ensures wider coverage across time and geographical locations. For studies of cyclic amplitudes in stars, this collective effort is crucial, as it allows for the meticulous tracking of variability patterns over extended periods—something that would be challenging for either professionals or amateurs alone.

2 Observation

We identified our candidate stars from the AAVSO International Variable Star Index (VSX), (Watson et al., 2006) by extracting BY Draconis stars that were deemed to be associated with M45 (Melotte 22) and the Alpha Persei Cluster (Melotte 20) for member stars brighter than 14.7 mag. Subsequently we extracted data with the same magnitude threshold from the All-Sky Automated Survey for Supernovae (ASAS-SN) online server (Kochanek et al, 2017), which is fed by a network of telescopes that monitor the whole sky for transient phenomena. This magnitude limit was imposed so as to use good quality data from the ASAS-SN sky survey (Shappee et al., 2014) because of its known reduced quality data in the V bandpass due to decreasing signal to noise ratio (SNR).

We then compared our star lists from VSX and ASAS-SN and identified stars that had divergent amplitude or period data. These stars were selected for further observation from our dedicated telescope network (ASPIRE, 2024) in order to mitigate any divergencies.

The search on VSX through these parameters yielded 36 candidate stars from M45, and 43 stars from the Alpha Persei cluster, amounting to a total of 79 BY Dra stars (Tables 1 and 2). While the VSX list provided most of the attributes that are pertinent to these stars, the

critical value of the rotation period for a number of these stars was missing. The data obtained from the ASAS-SN Survey was then used to derive the rotation period of these stars (hereafter referred to as PROT). The same data was also used to determine the cyclic period (P-CYC) that was unknown prior to this study.

This data obtained from the ASAS-SN server is made up of V and 'g' (SLOAN) magnitudes. In order to use data from both of these bandpasses, we adopted an offset for 'g' magnitudes of each star to align to the V (Johnson) data. The periods for all of our stars were derived through the Lomb Scargle (LS) algorithm (Scargle, 1982).

The observatories from the ASPIRE telescope network that participated in this study (ASPIRE, 2024) were Antares Observatory; Flarestar Observatory; Manikata Observatory; and Znith Observatory (all from Malta); Cerro del Viento Observatory (Spain); and Observatoire à la belle étoile (Canada). All observatories predominantly utilized Schmidt-Cassegrain Telescopes (SCT), except for the Canadian Observatory, which used a Maksutov telescope, with apertures ranging from 0.20 to 0.25 meters. A variety of cameras were employed, including models from SBIG, Moravian, Atik, and ASI, with pixel scales varying between 0.67 and 1.41 arcseconds per pixel and fields of view spanning from 25x17 to 46x31 arcminutes. All observatories used a V-bandpass filter, whereas Antares Observatory employed a clear filter whose data were calibrated to the V-bandpass (CV). Acquisition software across the network includes popular tools like Sequence Generator Pro (SGP), NINA, and MaximDL, reflecting a standardized yet flexible approach to astronomical data collection.

The data shown in Tables 1 and 2 contains information about candidate stars, including their coordinates, periods of variability, magnitudes, rotational periods, cyclical periods, absolute magnitudes and other attributes. Each row in the tables represents a star while the columns provide details about each star's characteristics. The columns cover attributes such as STAR (the stars name or identifier) COORD (coordinates) PERIOD (VSX) indicating the period of variability as listed in the Variable Star Index, MAG (AMP) denoting the magnitude and amplitude of the stars variability P ROT (d) representing the rotational period in days along with its associated error (P-ROT Error) AMP ROT for rotational variability amplitude measurements P-CYC (d) for cyclical period in days along, with its associated error (P-CYC Error) GMAG (Absolute) indicating the absolute magnitude of the star AMP CYC G (Mag) measuring amplitude for cyclical variability and BP-RP mag representing the color index of each star.

Tables 1 and 2 depict stars from our candidate list. The star's name that are in bold are stars that were observed by the ASPIRE Network where discrepancies between AAVSO's VSX and the ASASSN data were identified.

Table 1: BY Draconis Stars in M45 Cluster. The targets in bold are stars that were followed up by the ASPIRE Telescope Network. Precision of the Period (d) is according to the information found on VSX. (Data source: VSX). **Precision shown as stated by VSX.*

STAR	COORD (RA, DEC)	PERIOD (d)*	MAG (Amp) Bandpass (VSX)
V0810 Tau	03 43 02.94, +24 40 11.1	6.65058293	11.96 (0.075)V V
V0811 Tau	03 45 21.19, +23 43 39.0	0.42690081	12.68 (0.035)r V
V0812 Tau	03 46 04.12, +23 24 19.9	0.57988155	12.90 (0.125) V
V0813 Tau	03 46 06.50, +24 34 02.8	7.064627	12.81 (0.09) V
V0814 Tau	03 46 39.39, +24 01 46.9	6.41558	12.3 (0.075) V
V0815 Tau	03 47 13.53, +23 42 51.5	8.17841955	12.41 - 12.52 V
V0816 Tau *	03 51 53.38, +24 23 13.1	0.41747738	12.77 (0.109)r V
V0855 Tau	03 45 40.17, +24 37 38.1	0.532	10 (0.035) V
V0963 Tau	03 43 37.73, +23 32 09.5	3.887814	10.69 - 10.76 V
V0966 Tau	03 44 11.20, +23 22 45.6	2.60863382	11.41 - 11.54 V
V1038 Tau	03 44 20.09, +24 47 46.3	1.47850907	10.60 (0.048)r V
V1045 Tau	03 46 22.67, +24 34 12.5	3.08777064	10.41 (0.019)r V
V1085 Tau	03 45 35.40, +24 04 59.6	0.294	10.12 (0.05) V
V1089 Tau	03 49 24.05, +23 50 21.3	5.81926006	11.35 (0.011)r V
V1090 Tau	03 49 33.12, +23 47 43.4	4.88066973	10.93 (0.012)r V
V1168 Tau	03 44 04.84, +24 16 31.9	4.76537832	11.63 (0.16)V V
V1169 Tau	03 44 13.92, +24 46 45.8	3.92988991	10.79 (0.015)r V
V1170 Tau	03 44 26.28, +24 35 22.9	0.84290118	11.60 (0.023)r V
V1171 Tau	03 46 28.42, +24 26 02.2	1.32333028	11.10 (0.12)V V
V1172 Tau	03 47 38.00, +23 28 05.2	8.36686239	13.51 (0.12)V V
V1173 Tau	03 50 05.06, +24 07 26.5	6.43833028	14.02 (0.07) V
V1174 Tau	03 50 34.57, +24 30 28.2	5.15798051	12.65 (0.047)r V
V1175 Tau	03 50 40.07, +23 55 59.0	2.166659802	10.31 (0.07) V
V1176 Tau	03 50 54.33, +23 50 05.5	5.15798	11.57 (0.04) V
V1189 Tau	03 46 12.86, +24 03 15.8	1.39127	14.08 (0.14) V
V1193 Tau	03 51 12.08, +23 55 57.6	4.56183	14.86 (0.053)r V
V1227 Tau	03 45 44.54, +24 42 50.0	20.9	10.55 - 10.75 V
V1272 Tau	03 44 03.55, +24 30 15.2	1.476	10.762 (0.074) V
NSV 1354	03 49 25.13, +23 47 41.7	0.1460667	7.797 (0.006)r J
NSV 15742	03 42 48.92, +24 28 58.5	4.09844049	9.354 (0.013)r J

NSV 15744	03 43 34.40, +23 45 43.0	5.34002688	11.47 (0.018)r V
NSV 15766	03 46 10.05, +23 20 24.1	2.84578235	10.15 (0.016)r V
NSV 15772	03 46 53.26, +22 52 51.4	6.15460725	11.74 (0.021)r V
NSV 15785	03 48 34.50, +23 26 05.0	2.89109736	10.34 (0.017)r V
NSV 15789	03 48 58.49, +23 12 04.4	3.04122134	11.54 (0.014)r V
NSV 1300	03 47 24.59, +23 53 57.6	0.18762107	12.019 J (0.169)r V

Table 2: BY Draconis Stars in Alpha Persei Cluster. The highlighted targets are stars that were followed up by the ASPIRE Telescope Network. Precision of the Period (d) is according to the information found on VSX. (Data source: VSX). **Precision shown as stated by VSX.*

STAR	COORD (RA, DEC)	PERIOD (d)*	MAG (Amp) Bandpass (VSX)
V0484 Per	03 22 21.95, +49 08 27.7	n/a	11.66 - 11.75 V
V0485 Per	03 24 25.09, +48 48 21.8	0.641578	14.07 - 14.18 V
V0486 Per	03 26 27.62, +49 02 13.0	n/a	12.77 - 12.88 V
V0487 Per	03 27 23.29, +48 22 25.5	n/a	12.91 - 13.07 V
V0488 Per	03 28 18.65, +48 39 48.8	n/a	12.8 - 12.86 V
V0489 Per	03 30 22.48, +48 24 42.0	n/a	14.27 - 14.37 V
V0522 Per	03 18 27.39, +47 21 15.4	n/a	11.5 (0.15) V
V0523 Per	03 18 50.40, +48 16 04.0	n/a	12.59 (0.04) V
V0524 Per	03 18 58.65, +48 50 43.6	0.182855	13.44 (0.14) V
V0525 Per	03 19 02.76, +48 10 59.5	n/a	11.99 (0.1) V
V0526 Per	03 19 57.69, +49 52 07.5	n/a	12.37-12.64 V
V0527 Per	03 20 01.28, +46 53 02.0	n/a	12.57 (0.04) V
V0528 Per	03 21 16.04, +48 24 23.4	n/a	12.8 (0.18) V
V0529 Per	03 22 06.80, +47 34 06.5	n/a	12.0 (0.15) V
V0530 Per	03 03 24 48.35, +48 53 20.6	n/a	11.71 (0.09) V
V0532 Per	03 26 22.22, +49 25 37.5	0.492420	11.17 - 11.41 V
V0536 Per	03 28 48.44, +49 11 54.8	n/a	13.05 (0.2) V
V0537 Per	03 32 30.66, +49 10 35.3	n/a	11.98 (0.19) V
V0538 Per	03 03 32 51.07, +49 50 44.4	n/a	13.08 (0.08) V
V0539 Per	03 34 29.32, +49 21 44.1	n/a	13.24 (0.07) V
V0540 Per	03 36 22.00, +49 09 21.2	n/a	11.83 (0.11) V

V0541 Per	03 36 53.67, +48 23 58.7	n/a	12.45 (0.11) V
V0542 Per	03 40 33.89, +48 04 36.2	n/a	12.89 (0.04) V
V0625 Per	03 21 06.48, +48 26 13.7	n/a	12.8 (0.09) V
V0626 Per	03 21 22.18, +49 57 03.4	3.228381	13.89 (0.24) V
V0628 Per	03 26 25.33, +48 20 06.8	n/a	12.03 (0.07) V
V0629 Per	03 27 20.37, +47 59 25.1	4.313466	13.4 (0.22) V
V0630 Per	03 28 22.51, +49 14 30.2	n/a	12.78 (0.13) V
V0631 Per	03 28 23.72, +47 36 50.6	n/a	13.28 (0.08) V
V0688 Per	03 26 04.22, +48 48 07.1	0.7	10.65 - 10.71 V
V0689 Per	03 32 10.20, +49 08 29.5	0.645	11.99 - 12.11 V
V0700 Per	03 44 25.57, +32 12 30.0	8.41	13.57 (0.18) Ic
V0701 Per	03 44 26.63, +32 03 58.4	3.08	14.04 (0.18) Ic
V0767 Per	02 40 26.58, +42 45 40.1	7.242	14.16 (0.04) V
V0769 Per	02 40 30.38, +42 41 51.8	7.177	14.72 (0.04) V
V0770 Per	02 40 30.63, +42 51 01.6	10.759	14.16 (0.01) V
V0776 Per	02 40 48.91, +42 30 34.2	7.785	14.40 (0.06) V
V0782 Per	02 41 05.13, +42 56 43.1	4.996	14.65 (0.05) V
V0794 Per	02 41 33.44, +42 42 11.9	0.822	14.04 (0.02) V
V0796 Per	02 41 35.08, +42 33 31.0	2.509	14.23 (0.02) V
V0797 Per	02 41 35.25, +42 41 02.5	0.893	14.63 (0.10) V
V0800 Per	02 41 38.14, +42 44 04.4	1.181	14.15 (0.01) V
V0804 Per	02 41 44.17, +42 46 07.6	6.674	14.56 (0.02) V
V0840 Per	02 42 21.89, +42 32 13.0	6.837	14.27 (0.03) V
V0864 Per	02 42 50.77, +42 58 07.8	0.946	14.75 (0.09) V
V0867 Per	02 42 56.90, +42 35 21.9	6.076	14.52 (0.06) V
NSV 1130	03 25 01.50, +54 14 36.7	3.6978	11.86 - 11.94 V

3 Data analysis

3.1 Homogeneity amongst our candidate list.

In order to uncover any differences amongst the chosen stars of the two clusters, we obtained further data about their Absolute G MAG from the GAIA DR 3 (Gaia Collaboration, 2020). The GMAG refers to the absolute magnitude MG that is derived from the GSP-Phot Aeneas from the MARCS library using BP/RP spectra. The Box Plot in fig. 1 shows the GMAG

values for our star sample derived from M45 and the Alpha Persei. As our dataset pair contained an unequal number of stars, the plot generated for each group was adjusted to compensate for this difference. Fig. 1 shows the median, mean (represented by the triangle) and interquartile range showing the spread of the middle 50% of a dataset to help us identify outliers in both groups.

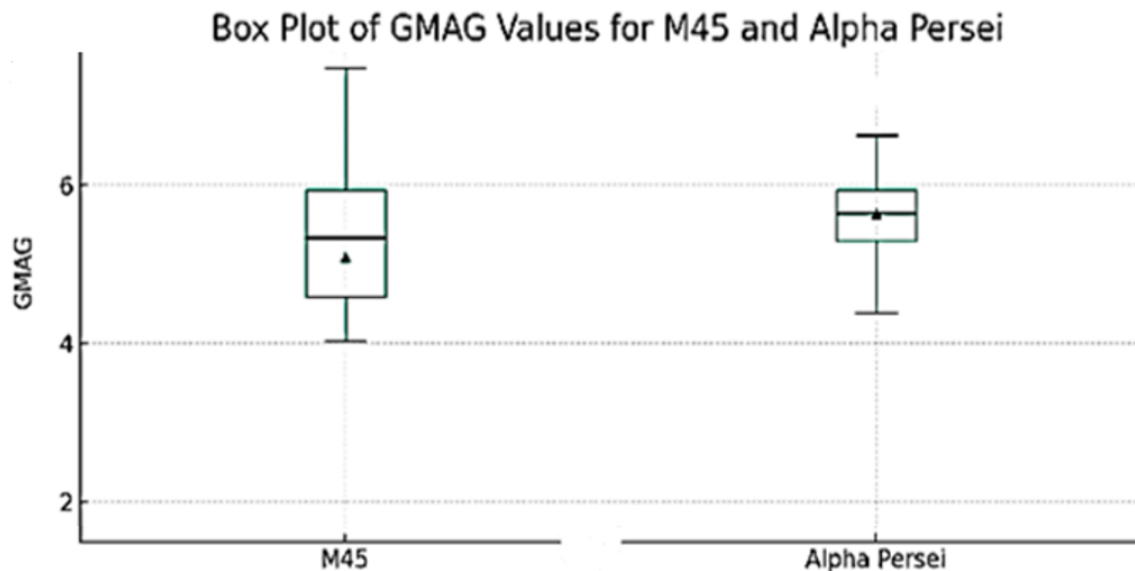


Figure 1: A GMAG (abs) Box Plot of the BY Draconids sample stars from M45 and the Alpha Persei cluster.

Results shown in fig. 1 suggest that the median GMAG values for both star groups are situated around the middle of the data range, with the triangles indicating the means are close to the medians. This outcome implies that our sample comprises a somewhat symmetric distribution for both groups. In addition, the ranges are relatively small for both groups, indicating that the middle 50% of the stars in each group have similar GMAG values. This outcome was expected as the stars belong to the same class of variable stars. The range values are seen to be slightly wider for M45 stars than those from Alpha Persei suggesting that the former stars have a wider variation in absolute GMAG.

3.2 Periodicity analysis.

Throughout our analysis we have used the Lomb Scargle periodogram (Scargle, 1982) for the detection and characterization of periodic solutions. We have preferred this algorithm over the Generalized Lomb-Scargle (GLS) especially because when periods are significantly longer than the available observational window (data range), such as for Period Cycle (P-CYC) of BY Draconis stars, the GLS's floating mean model can misinterpret trends or gaps in data as part of the signal, leading to unstable or "open" solutions. The Lomb Scargle periodogram

avoids this by relying on stricter assumptions that fit better in such scenarios (VanderPlas, 2018).

4 Results

4.1. Stellar variability in BY Draconis Stars: Rotation and activity cycle findings.

Table 3 presents the results for the candidate stars from our list as derived from the Lomb-Scargle periodogram analysis for the following attributes: PROT (rotation period in days), standard error (in days), amplitude (AMP-R), epoch, PCYC (period cycle in days in HJD), amplitude (AMP-C), and epoch.

Two amplitude values are provided in the table because of the fact that the PROT data was normalized to a standard reference point. This normalization compensates for gradual brightness variations associated with the PCYC. As a result, the amplitudes corresponding to PROT are generally lower than those for PCYC that show the total amplitude through both processes. This approach allows for more accurate determination of the true amplitude generated by the rotation period, effectively isolating it from brightness variations induced by the PCYC processes.

Table 3: Periodicity results for the Rotation Period (PROT) and Cyclic Period (PCYC) for star candidates from M45 and Alpha Persei (Data source: VSX).

Star	PROT (d)	Error	Amp-R	Epoch (HJD)	PCYC (d)	AMP-C	Epoch
V0810 Tau	6.629485	0.002093	0.039	2458888.788	1724.1	0.021	2459831.0
V0811 Tau	0.42776	0.001084	0.014	2457694.878	9452.5	0.104	2456215.1
V0812 Tau	0.581256	0.000331	0.022	2457358.809	3335.6	0.062	2458346.9
V0813 Tau	7.030574	0.004056	0.031	2458087.710	5717.6	0.111	2456998.9
V0814 Tau	6.085781	0.004703	0.022	2459135.984	1063.2	0.031	2459130.9
V0815 Tau	7.592557	0.006588	0.017	2459267.538	1981.9	0.030	2458023.8
V0816 Tau	0.417072	0.000523	0.070	2457321.049	4429.3	0.177	2459526.1
V0855 Tau	0.49896	0.000115	0.035	2458352.017	8395.9	0.034	2456477.1
V0963 Tau	3.913611	0.003971	0.030	2459818.857	3733.0	0.051	2459233.7

V0966 Tau	2.594673	0.00096	0.022	2459168.610	3467.5	0.058	2456883.1
V1038 Tau	1.480245	0.001036	0.027	2458129.887	4262.0	0.099	2457671.9
V1045 Tau	3.09119	0.001593	0.007	2459519.724	1182.1	0.023	2459247.7
V1089 Tau	5.567312	0.002215	0.019	2459913.301	2348.1	0.034	2458488.9
V1090 Tau	4.706292	0.005742	0.010	2458684.942	2258.9	0.046	2458383.8
V1168 Tau	4.748505	0.028394	0.024	2459424.916	3285.2	0.052	2459769.1
V1170 Tau	0.846696	0.001405	0.019	2459903.526	1705.4	0.085	2455946.8
V1171 Tau	1.31689	0.000523	0.017	2459404.095	4141.3	0.048	2459588.8
V1172 Tau	8.330248	0.004626	0.051	2458538.510	1821.0	0.042	2456576.0
V1173 Tau	6.291845	0.002707	0.035	2459459.655	3460.0	0.076	2458343.7
V1174 Tau	5.158507	0.086120	0.032	2459819.611	3602.2	0.049	2458427.9
V1175 Tau	2.180089	0.002564	0.011	2459600.622	2753.3	0.024	2458151.3
V1176 Tau	5.100306	0.002001	0.019	2459991.545	1230.5	0.025	2458814.8
V1189 Tau	1.38862	0.000987	0.045	2459216.666	3226.4	0.110	2457948.1
V1193 Tau	4.579376	0.012427	0.036	2459178.904	2884.5	0.050	2455988.7
V1227 Tau	19.829824	0.227830	0.029	2458452.006	2532.3	0.025	2459145.9
V1272 Tau	1.475755	0.000242	0.026	2459793.084	3444.1	0.101	2459813.6
NSV 15789	6.134969	0.013550	0.014	2459882.472	2544.6	0.019	2458729.8
NSV 15772	6.106870	0.018647	0.013	2458436.663	2314.7	0.027	2458112.7
NSV 15766	2.854241	0.001883	0.013	2459984.568	3801.9	0.019	2458900.5
NSV 15744	5.278094	0.006440	0.015	2456215.120	1285.5	0.045	2459857.5
NSV 15742	3.994887	0.009247	0.007	2459598.359	2075.0	0.006	2457658.0
NSV 1354	13.935811	0.000110	0.029	2458414.566	1151.5	0.096	2457410.8

NSV 1300	0.230681	0.000692	0.069	2458888.278	5173.7	0.224	2457053.7
NSV 1130	3.584372	0.005282	0.011	2457581.120	1063.5	0.018	2458800.0
V0484 Per	1.539301	0.001357	0.028	2455937.781	1662.3	0.044	2455937.8
V0485 Per	1.795977	0.006881	0.051	2458477.854	2792.3	0.128	2458801.9
V0486 Per	0.359691	0.00317	0.040	2458831.836	1774.5	0.062	2457007.8
V0487 Per	0.209468	0.00066	0.0455	2459288.617	2299.0	0.049	2459488.0
V0488 Per	5.608811	0.018017	0.028	2459830.806	1750.9	0.047	2459062.9
V0489 Per	0.21727	0.000270	0.0655	2458858.78	4682.3	0.050	2457007.8
V0522 Per	2.596593	0.002158	0.021	2459466.004	1668.8	0.071	2459476.0
V0523 Per	2.362949	0.001675	0.030	2459506.908	4560.4	0.132	2457007.8
V0524 Per	0.182843	0.000028	0.0354	2458837.821	4573.6	0.079	2458145.8
V0525 Per	0.637400	0.002449	0.028	2459436.883	4469.9	0.110	2460212.8
V0526 Per	0.351914	0.000427	0.183	2460291.307	4738.5	0.130	2460279.9
V0527 Per	18.820577	0.184978	0.015	2457007.835	4767.2	0.069	2457659.0
V0528 Per	5.207128	0.01416	0.031	2458731.957	4573.6	0.062	2457638.1
V0529 Per	0.259235	0.000328	0.022	2459144.766	4500.7	0.080	2457007.8
V0530 Per	0.321014	0.006867	0.036	2459078.119	2633.8	0.063	2459132.0
V0532 Per	0.491795	0.001604	0.050	2455937.781	1792.3	0.117	2458312.0
V0536 Per	0.896521	0.002444	0.055	2460312.345	4444.8	0.079	2459644.7
V0537 Per	15.313936	0.023452	0.024	2460220.870	4383.0	0.085	2459621.7
V0538 Per	3.725782	0.004164	0.031	2459970.785	3407.7	0.075	2459669.6
V0539 Per	6.891799	0.014249	0.030	2458118.895	4547.3	0.092	2460264.8
V0540 Per	0.247402	0.000367	0.100	2457948.112	3069.5	0.065	2458853.7

V0541 Per	0.223214	0.000299	0.080	2460265.212	4627.3	0.079	2458152.8
V0542 Per	19.952115	0.12208	0.031	2459600.841	4796.2	0.203	2457409.8
V0625 Per	5.860291	0.010532	0.052	2459664.593	4426.0	0.111	2459827.9
V0626 Per	0.590145	0.008533	0.041	2459089.980	4724.3	0.325	2457753.9
V0628 Per	0.831808	0.004567	0.029	2460240.809	3385.7	0.059	2457007.8
V0629 Per	4.314447	0.010785	0.039	2458385.902	3422.5	0.111	2459213.8
V0630 Per	6.185335	0.022167	0.038	2459464.878	838.2	0.027	2458434.9
V0631 Per	5.157358	0.057126	0.027	2460156.922	1546.2	0.057	2460266.0
V0688 Per	5.505850	0.034104	0.031	2460213.878	3893.4	0.142	2458849.8
V0689 Per	0.298939	0.000269	0.100	2457007.847	2156.6	0.029	2457997.1
V0700 Per	8.372182	0.050181	0.174	2457989.087	2473.7	0.429	2459052.1
V0701 Per	17.730496	0.027944	0.088	2460229.73	5839.3	0.230	2457642.9
V0767 Per	5.662372	0.008051	0.014	2458352.848	3893.4	0.034	2457305.1
V0769 Per	7.206027	0.02974	0.022	2459916.681	3266.5	0.028	2457223.1
V0770 Per	8.561644	0.029321	0.017	2459931.726	3712.4	0.025	2459070.0
V0776 Per	8.178358	0.038753	0.018	2458421.826	2965.6	0.029	2458383.1
V0782 Per	6.900518	0.007936	0.017	2457007.835	3730.0	0.042	2457008.8
V0796 Per	1.829491	0.004351	0.018	2458340.034	2445.9	0.029	2457007.8
V0797 Per	8.804931	0.044402	0.033	2458450.777	4004.6	0.074	2457008.8
V0800 Per	5.495311	0.003221	0.017	2458804.776	2140.5	0.014	2458731.0
V0804 Per	1.307108	0.000447	0.069	2459196.815	1276.3	0.054	2458348.0
V0840 Per	3.046304	0.002846	0.015	2458402.737	1537.5	0.020	2459907.6
V0864 Per	7.849294	0.018894	0.033	2458559.612	4322.9	0.153	2457967.0

V0867 Per	14.665102	0.059436	0.019	2458705.880	2822.3	0.028	2458782.8
-----------	-----------	----------	-------	-------------	--------	-------	-----------

The histogram in figure 2 depicts the rotation period (PROT) of the candidate stars for both clusters. For our candidate star list, the histogram shows clear differences in the PROT distributions of the M45 and Alpha Per cluster. Alpha Per has a strong concentration of rapidly rotating stars with very short periods, contrasting with the more evenly distributed rotation speeds in M45.

In the intermediate range, M45 exhibits a broader spread of stars, while Alpha Per shows a noticeable gap, indicating fewer stars in this category. For longer rotation periods, Alpha Per reveals a distinct secondary peak of slower rotators, unlike M45, which has few stars in this range.

Overall, Alpha Per displays a bimodal pattern with peaks among fast and slow rotators, reflecting a more diverse population. In contrast, M45 shows a more uniform distribution centered on moderate rotation speeds that is perhaps due to differences in the clusters' stellar age and dynamics.

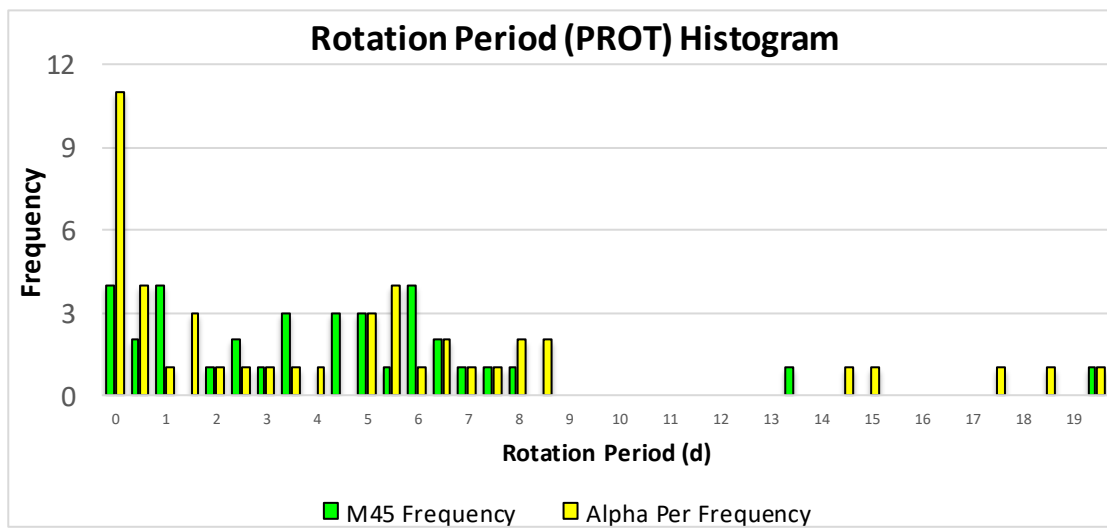


Figure 2: Histogram of the Rotation Period (PROT) for candidate stars in the Alpha Persei Cluster (in yellow) and M45 Cluster (green).

4.2. Key insights on the rotational period and characteristics of the candidate BY Draconis Stars.

Our analysis of the data provides an insight into the critical attributes derived for the BY Draconis stars in our candidate list. The features we looked into include the rotation periods (PROT), amplitude of rotational variations (AMP-R), cyclic periods (PCYC), and amplitude of cyclic variations (AMP-C).

4.2.1. Rotation periods (PROT).

The rotation periods (PROT) of stars in both clusters range from 0.17 days (for V0487 Per) to a long PROT of 19.95 days (for V0542 Per). This is in line with what Chahal et al., (2022) have observed in that younger stars rotate faster than older ones. This spin-down phenomenon is exhibited with increasing age as the loss of angular momentum induced by magnetized winds and structural variations leads to a decrease in the stellar rotational speed, reducing the dynamo efficiency that leads to reduced magnetic activity. This explains why young stars are expected to exhibit fast rotation with associated enhanced magnetic activity.

The data derived from our candidate stars support this trend, as the average rotation derived from a 45-star sample of Alpha Persei stars was estimated as 4.942 d. The age of the Alpha Persei cluster is estimated to be around 79 million years old while that of M45 has an estimated age of approximately 127.4 million years (Boyle & Bouma, 2023). For our 35-star sample located in M45 we obtained an average rotation period (PROT) of 4.588 d. These values align themselves well with the spin-down theory as Alpha Persei's Star Cluster is younger than M45. It is interesting to note that Boyle and Bouma (2023) state that the rotation periods of stars, which are indicators of stellar rotation, typically become well-defined in open clusters at ages exceeding 100 million years (Myr), as magnetic spin-down stabilizes the initial stellar spin rate, enabling methods like gyrochronology. Boyle and Bouma (2023) add that with regards to young stellar clusters, stars with masses of approximately 0.8 times the mass of the Sun (M_{\odot}) exhibits rotational behavior that is beginning to converge into a well-defined slow sequence. This is relevant to BY Draconis stars which typically have masses between 0.1 and 1.3 solar masses (M_{\odot}). This convergence indicates the onset of the magnetic braking process that slows down stellar rotation over time. However, Boyle & Bouma (2023) state that the process of rotational braking, becomes effective for stars above a mass threshold of $0.8 M_{\odot}$, at around 80 million years. In consideration that Alpha Persei has an estimated age of 79 M years, the formation of these slow sequences remains incomplete at this age and additional processes will be exhibited as the cluster evolve through time.

4.2.2. The cyclic period (PCYC).

Using the Lomb-Scargle periodogram method we conducted a period search to uncover the Cyclic Period (PCYC) of BY Draconis stars from our candidate list. The PCYC is thought to be related to their long-term magnetic activity cycles, analogous to the solar sunspot cycle. These are driven by stellar magnetic activity cycles, which can range from a few years to several decades (Chahal et al. 2022). Similar to the Sun's ~11-year sunspot cycle, BY Draconis stars exhibit periodic variability in brightness due to evolving starspots and faculae on their surfaces. However, the periodicity of PCYC can vary widely among the BY Draconis stars from a few years to several decades that may in turn be influenced by the mass of the star, rotation rate, and magnetic field strengths (Chahal et al. 2022).

Figure 3 is a histogram plot showing the frequency of Period Cycles (PCYC) of all the BY Draconis type stars we analysed from both M45 and Alpha Persei star clusters.

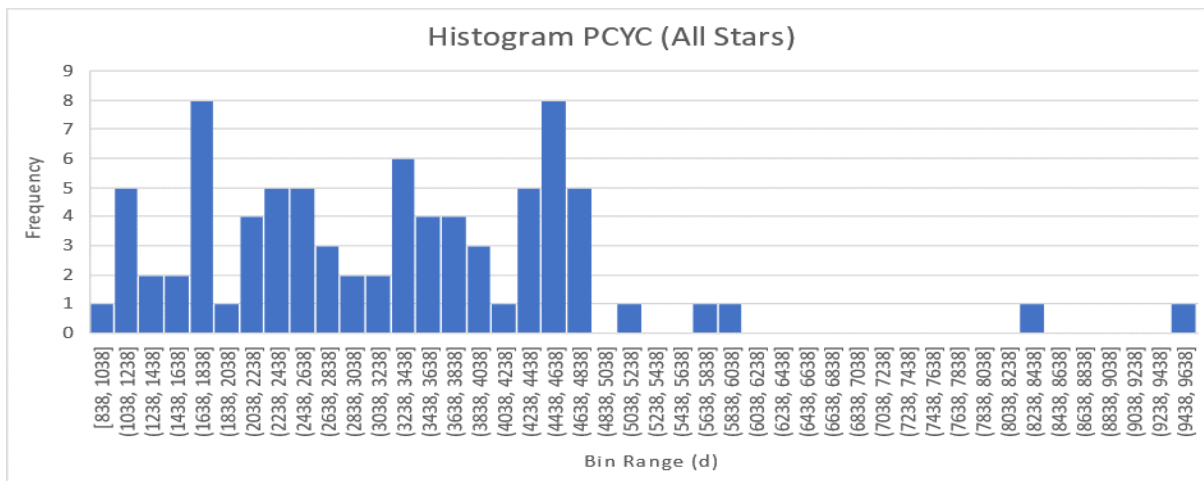


Figure 3: Histogram showing the frequency of Period Cycles (PCYC) of all the stars analysed from both M45 and Alpha Persei clusters.

4.2.3. Comparative analysis.

This comparative analysis of key attributes offers insights into potential correlations among BY Draconis star parameters, including rotation period (PROT) versus rotational amplitude (AMP-R) and cyclic period (PCYC) versus cyclic amplitude (AMP-C). These comparisons can shed light on the periodic magnetic activity, stellar evolution, and magnetic cycle dynamics of BY Draconis stars (Chahal, 2022). For example, high AMP-R values indicate stronger magnetic fields and prominent star spot coverage - traits commonly associated with younger, faster-rotating stars. In contrast, older stars with longer PROT and lower AMP-R values reflect gradual angular momentum loss and diminished magnetic activity, likely caused by magnetic braking as the stars evolve. An examination of the correlation between PCYC and AMP-C can reveal valuable information about the diversity in magnetic cycle behaviors among these stars, highlighting differences in cycle duration and amplitude that underscore the complexity of magnetic field generation in low-mass stars. Furthermore, stars with PCYC values comparable to the Sun's ~ 11 -year cycle but exhibiting higher AMP-C amplitudes can suggest a more efficient dynamo mechanism than their solar counterparts. The objective of this part of the study is therefore to provide valuable insights into the physical processes driving the magnetic and rotational dynamics of BY Draconis stars.

With reference to outliers shown in some of the diagrams, it is pertinent to note that these stars were classified as BY Dra stars. In fact, attributes such as the cyclic period (PCYC) that is exhibited by this class of variable stars have been uncovered. The authors did not find any empirical reason to strike off these 'outlier' stars. Their inhomogeneity may be due to the stars being binary stars. It is known that BY Draconis stars can also be binaries (Chahal, 2022) and when adopting parameter comparison through a whole data set, the presence of outliers is expected.

4.2.3.1. Relation between rotational amplitude (AMP-R) and rotational period (PROT).

The relationship between AMP-R and PROT is expected to reflect the connection between stellar rotation and magnetic activity, where faster rotators with higher AMP-R values typically exhibit stronger magnetic fields and larger, more unevenly distributed starspots, indicative of intense surface activity (Chahal et al., 2022). Conversely, slower rotators with lower AMP-R values show the gradual decline in magnetic activity due to rotational braking over time. However, our results suggest that this relationship is not straightforward across all BY Draconis stars, possibly due to differences such as those exhibited in evolutionary stages and internal magnetic field structures.

Our correlation analysis between rotation period (PROT) and rotational amplitude (AMP-R) across all BY Draconis candidate star list reveals a weak negative correlation which is not statistically significant (fig. 4; $r = -0.10$, $p = 0.373$). This suggests that our candidate stars do not present a fundamental relationship between rotational speed and the amplitude of brightness variations due to starspots. While AMP-R represents brightness variations caused by rotational variation, where amplitude is determined by the number and distribution of starspots on the stellar disk, the wide scatter in the data indicates that other factors such as stellar age, binarity, inclination angle, and variations in star spot coverage might be in play at shaping the observed amplitudes.

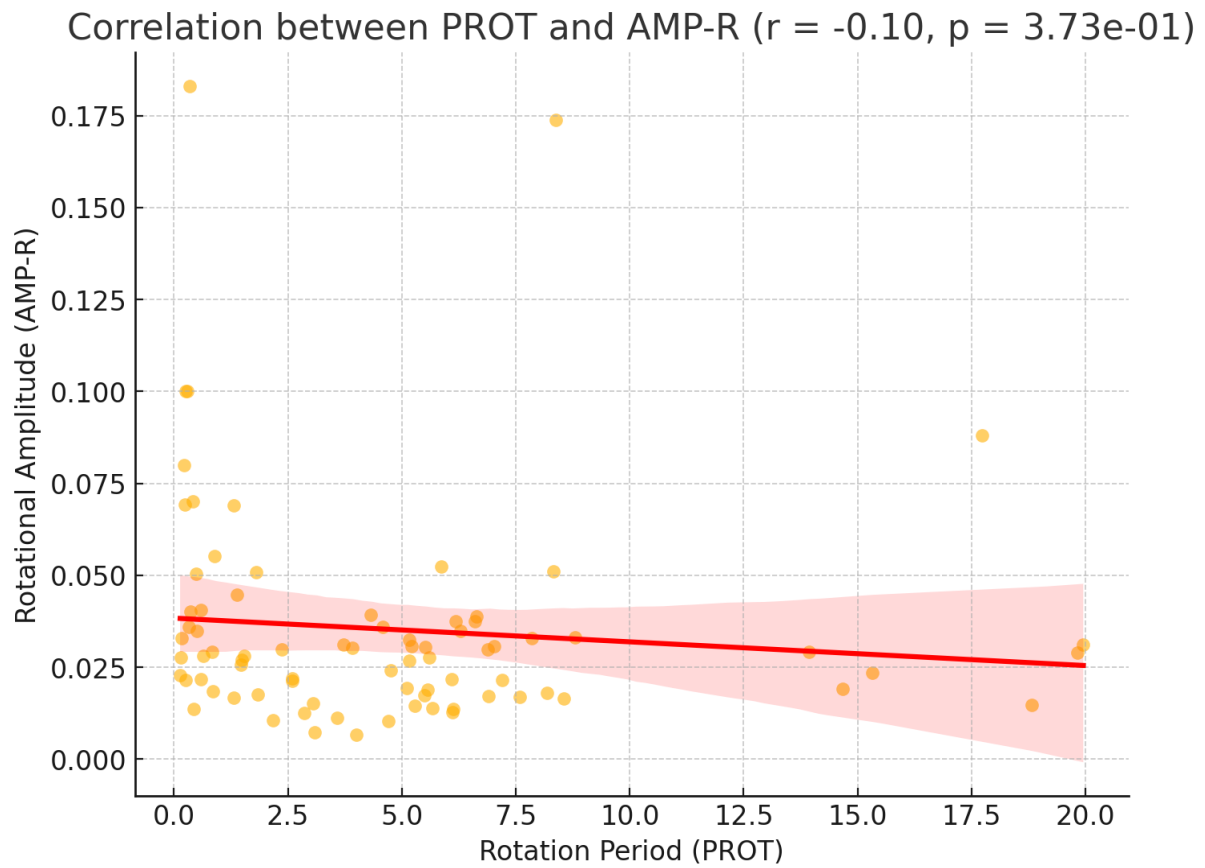


Figure 4: Rotational Amplitude against Rotation Period with sampled stars from both Alpha Persei and M45 clusters.

M45 Cluster: Correlation between PROT and AMP-R ($r = 0.07$, $p = 7.39e-01$)

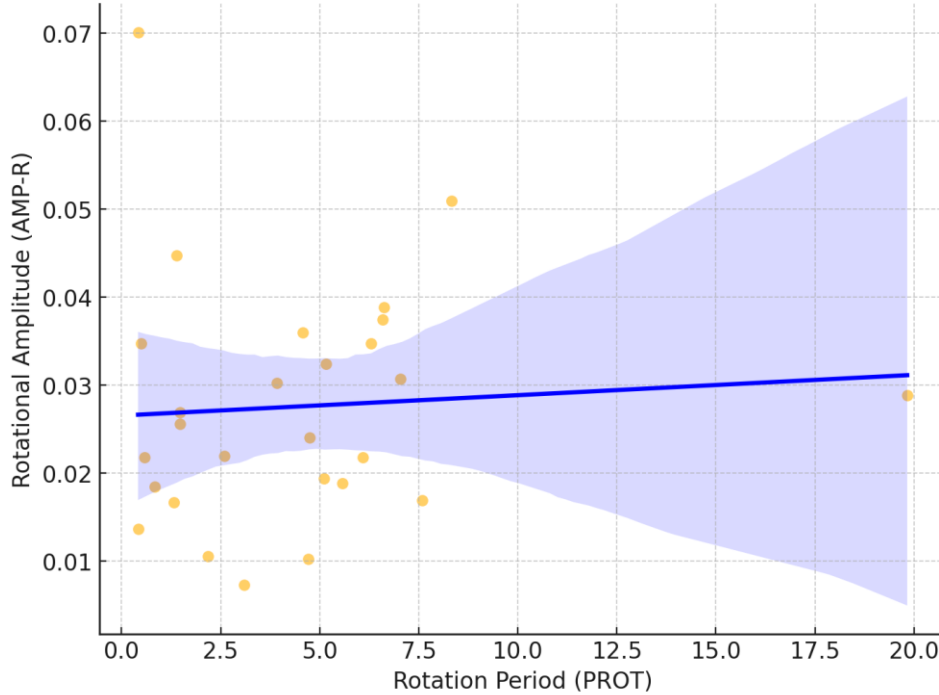


Figure 5: Rotational Amplitude against Rotation Period for sampled stars from the M45 cluster.

Alpha Persei Cluster: Correlation between PROT and AMP-R ($r = -0.14$, $p = 3.70e-01$)

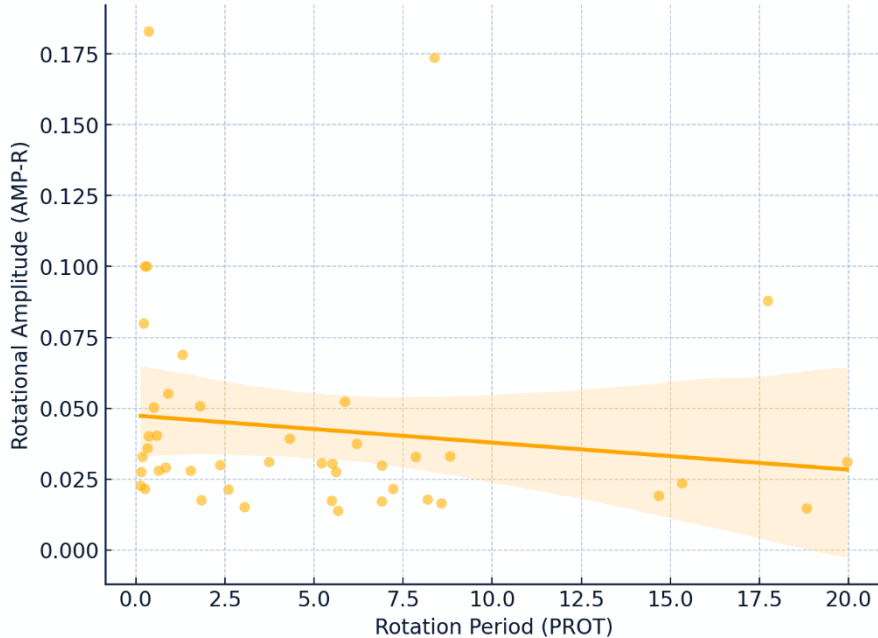


Figure 6: Rotational Amplitude against Rotation Period for sampled stars from Alpha Persei cluster.

The cross correlation of the AMP-R vs. PROT relationship for the star candidates from the individual clusters are shown Figures 5 and 6). The M45 dataset shows a statistically non-

significant, very small negative relationship ($r = -0.03$, $p = 0.846$), suggesting that possibly, in this relatively older cluster, magnetic cycles are more stable, and that rotational amplitude variations are not strongly influenced by spin rate. In contrast, Alpha Persei exhibits a stronger negative correlation ($r = -0.13$, $p = 0.364$), implying that faster rotators may exhibit slightly higher rotational modulation (as inferred by Chahal, 2022), though the scatter in the data indicates statistical insignificance, that is possibly limited by our small sample size or perhaps that other stellar properties may be having a more significant role. The weaker correlation in M45 further supports the idea that differing evolutionary processes between the two clusters are influencing how rotational amplitude changes with spin rate.

These findings at face value, show that stellar magnetic activity is complex, and rotational amplitude is not just controlled by rotation period. Instead, it is likely influenced by a mix of stellar age, binary star systems, changes in the star's dynamo, and magnetic field behavior.

4.2.3.2. Insight into cyclic amplitude (AMP-C) Variations.

As previously mentioned, the Cyclic Amplitude (AMP-C) generated by the long-term magnetic activity cycles (PCYC) in BY Draconis stars is an important parameter that quantifies the magnitude of brightness fluctuations. The PCYC closely resembles the Sun's approximately 11-year sunspot cycle (Jeffers et al., 2023). The Cyclic Amplitude (AMP-C) is fundamentally linked to the presence of star spots on BY Draconis stars which manifest as cooler, darker regions across the stellar surface. These spots result from the complex interaction between stellar magnetic fields and surface convection, leading to variations in the star's overall brightness as it changes over time.

Just as the Sun's cycle impacts solar phenomena like flares and coronal mass ejections (CMEs) (Charbonneau, 2010), the cyclic period amplitude (AMP-C) in BY Draconis stars offers insights into the intensity and evolution of magnetic activity over time. However, studies indicate that the magnetic cycles in BY Draconis stars can differ significantly from the solar example due to their rapid rotation, convective envelopes, and binarity (Chahal et al., 2022). Faster rotation rates in BY Draconis stars are thought to enhance the dynamo mechanism, leading to a stronger and shorter magnetic cycle compared to the Sun.

4.2.3.3. The cycle amplitude (AMP-C).

Figures 7 to 9 show the correlation between cyclic amplitude (AMP-C) and cyclic period (PCYC) for BY Draconis stars in both Alpha Persei and the M45 clusters, highlighting a statistically significant, moderately positive correlation across the dataset ($r = 0.35$, $p = 0.0016$). This trend aligns with dynamo theory (Charbonneau, 2010), which suggests that stronger magnetic fields (that induce higher AMP-C values due to the enhanced prevalence of star spots) require more time to complete a full magnetic cycle, leading to longer PCYC values (Chahal et al., 2022). This relationship is particularly pronounced in the M45 dataset ($r = 0.44$, $p = 0.022$), where stars with prolonged cyclic activity exhibit stronger brightness

variations over time, possibly due to more structured and persistent magnetic field fluctuations. In contrast, Alpha Persei ($r = 0.33$, $p = 0.024$) shows a slightly weaker but still significant correlation, suggesting that in this younger cluster, magnetic activity cycles are still evolving and stabilizing. Observational data from Kepler and TESS, as well as studies of late-type stars, confirm that highly active BY Draconis stars with pronounced variability tend to have longer magnetic cycles (Oláh et al., 2022), supporting further the models of stellar magnetism and dynamo evolution. These findings support the idea that magnetic energy in BY Draconis stars affects how strong and how long their brightness changes last (Chahal et al., 2022 & Oláh et al., 2022), providing key insights into the interplay between rotation, magnetic cycles and stellar evolution.

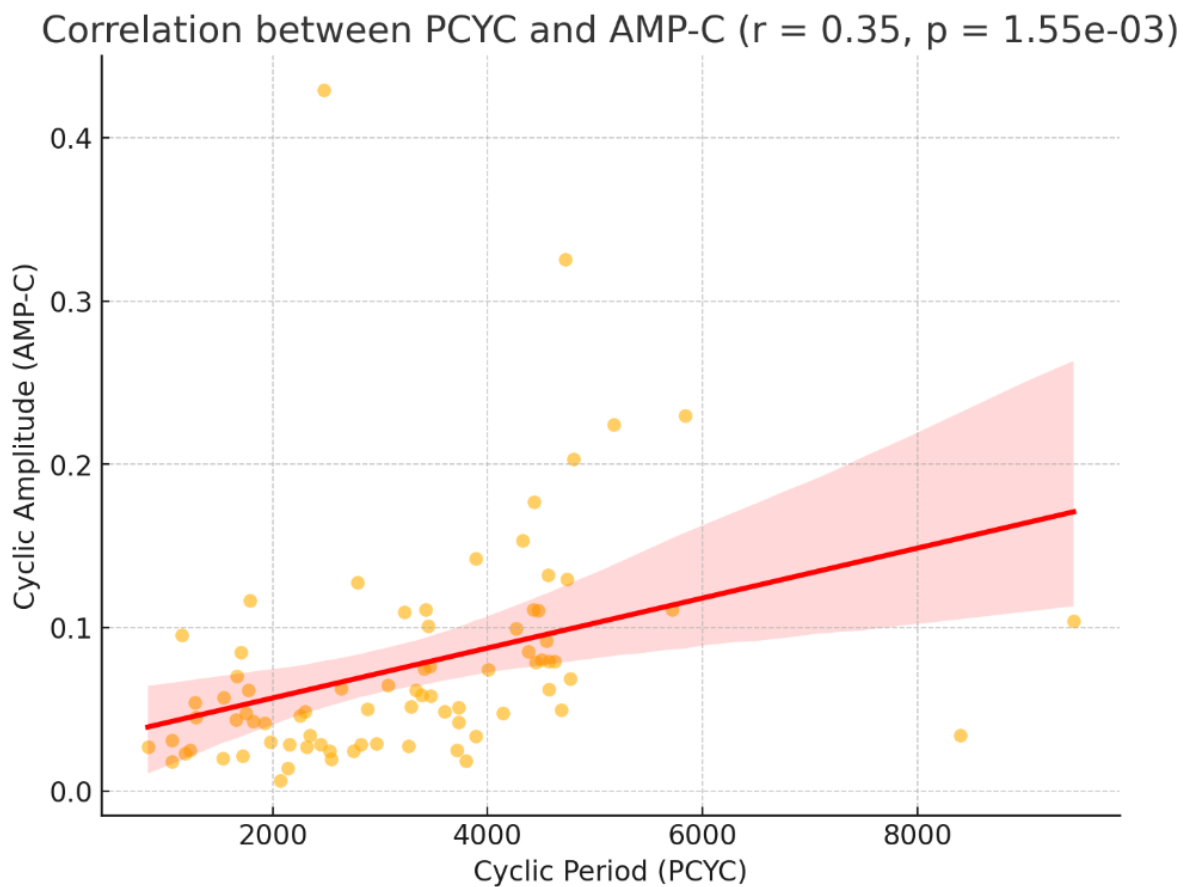


Figure 7: Amplitude of the cycle period against the Cycle Period (PCYC) for BY Draconis sampled stars in the Alpha Persei and M45 clusters.

M45 Cluster: Correlation between PCYC and AMP-C ($r = 0.44$, $p = 2.15e-02$)

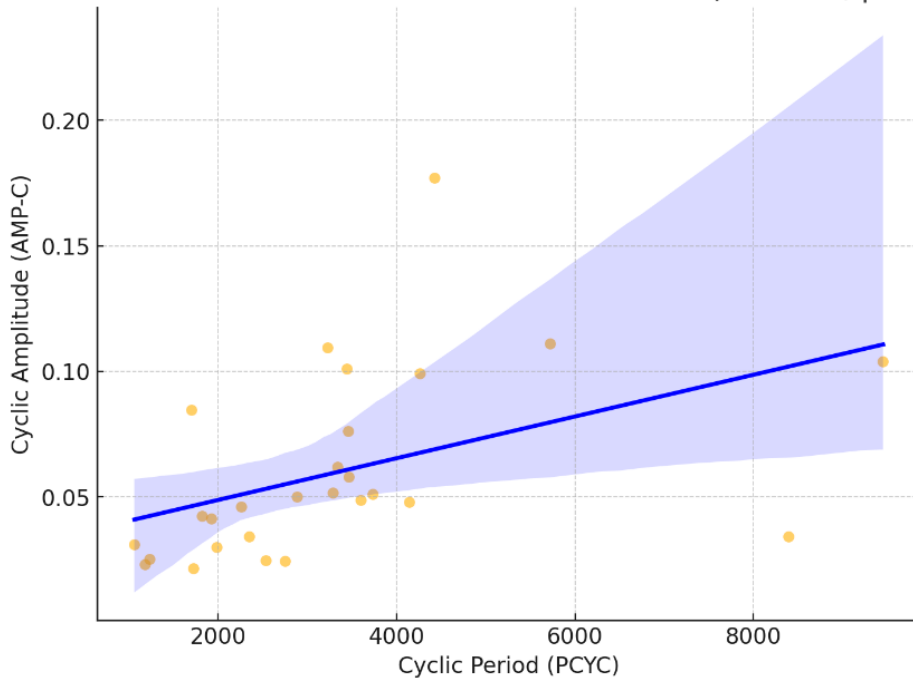


Figure 8: Amplitude against the Cycle Period (PCYC) for BY Draconis sampled stars in the M45 cluster.

Alpha Persei Cluster: Correlation between PCYC and AMP-C ($r = 0.33$, $p = 2.85e-02$)

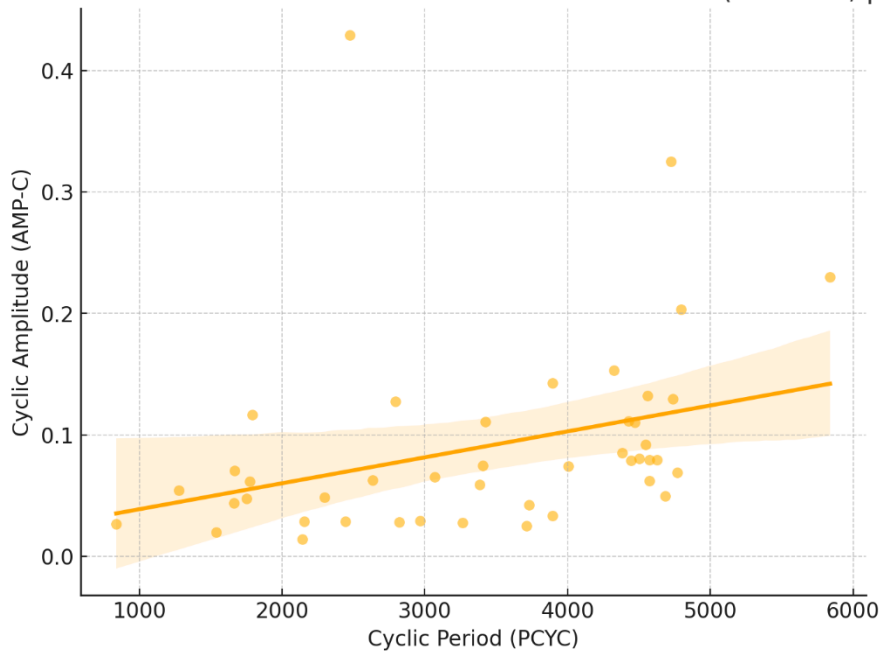


Figure 9: Amplitude against the Cycle Period (PCYC) for BY Draconis sampled stars in the Alpha Persei Cluster.

4.2.3.4. Correlation between the cyclic period (PCYC) and rotational period (PROT).

The combined data from both clusters (fig. 12) show that there is a statistically non-significant, very small negative relationship between PROT and PCYC (fig. 10; $r = -0.03$, $p = 0.8149$). The magnitude of the relationship between rotation period (PROT) and cyclic period (PCYC) also differs between the candidate stars in the M45 (fig.10) from those in the Alpha Persei cluster (fig.11), a result which could be attributed to their distinct evolutionary stages.

In the case of the candidate stars in the M45 cluster, there is a weak but statistically significant, negative correlation (fig. 10; $r = -0.36$, $p = 0.0628$), suggesting that stars with longer rotation periods tend to have shorter cyclic periods. This trend possibly arises from magnetic braking, where older stars experience rotational slow-down, altering their magnetic cycles. In contrast, our Alpha Persei candidate stars exhibit a statistically significant weak positive correlation (fig. 11; $r = 0.31$, $p = 0.0428$), indicating that stars with longer rotation periods tend to have longer cyclic periods. This suggests that in consideration that the Alpha Persei cluster is considerably younger than M45, the dynamo-driven relationship between rotation and magnetic cycles might still be evolving, and show a lesser influence from braking effects. These results highlight how stellar age and rotational dynamics can shape the long-term magnetic variability, with the older stars in M45 showing signs of rotational evolution through enhanced magnetic braking, whilst the younger Alpha Persei stars retain a more direct link between their rotation rates and magnetic cycles.

M45 Cluster: Correlation between PROT and PCYC ($r = -0.36, p = 6.28e-02$)

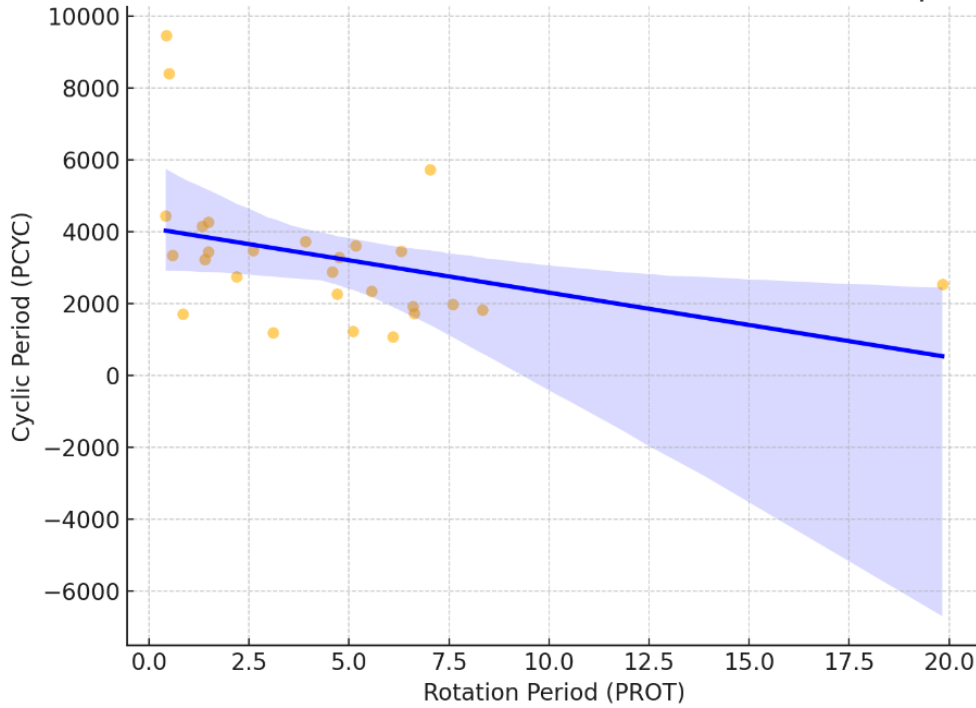


Figure 10: Amplitude against the Cycle Period (PCYC) for BY Draconis sampled stars in the M45 Cluster.

Alpha Persei Cluster: Correlation between PROT and PCYC ($r = 0.31, p = 4.28e-02$)

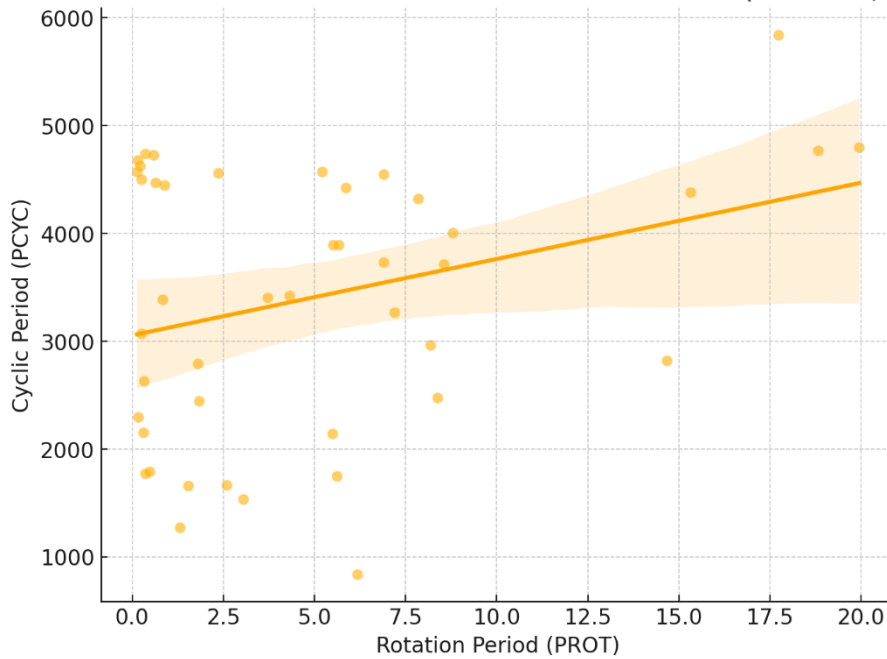


Figure 11: Correlation between PROT and PCYC in the Alpha Persei cluster showing a positive correlation suggesting that the longer the rotation period is, the longer is the cyclic period.

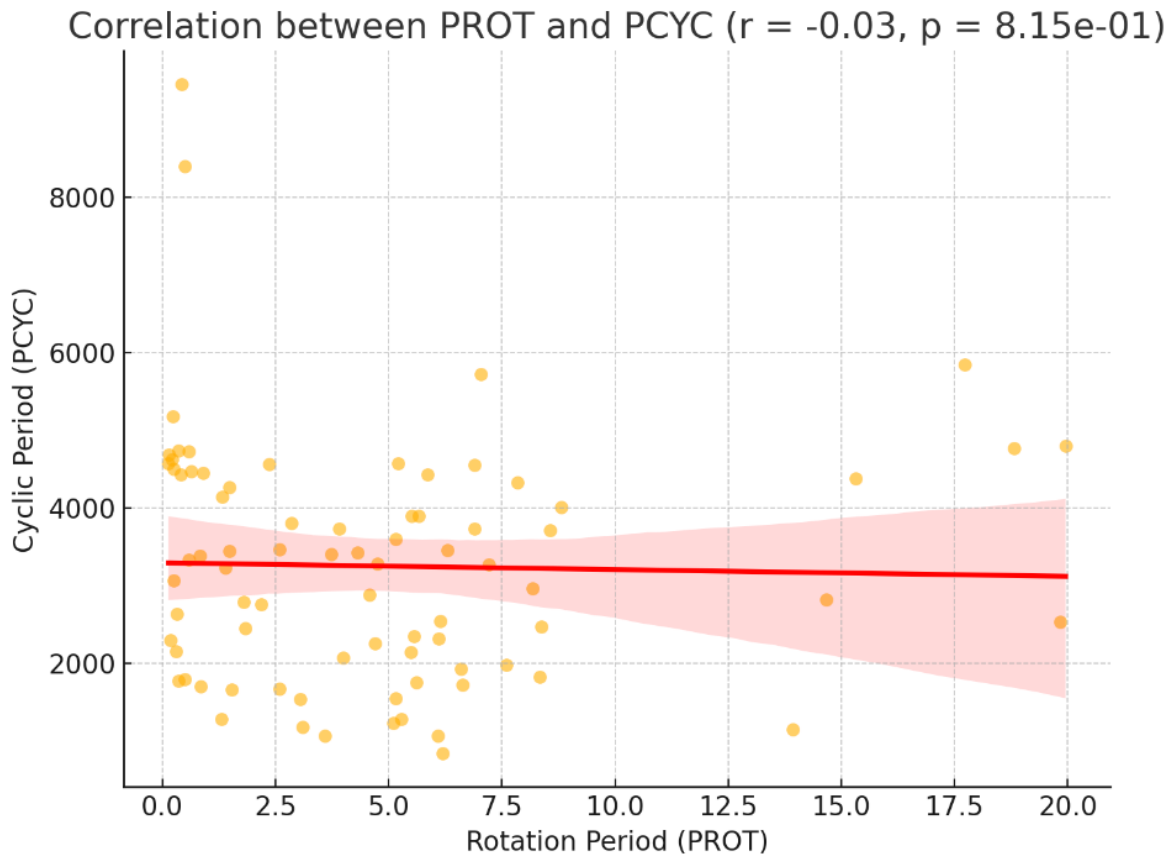


Figure 12: Correlation between PROT and PCYC in both clusters showing a negligible negative correlation indicating that the combination of data from both clusters has nullified their trends. This is likely due to the different ages where the spin-down effects have played a significant role.

4.2.3.5. Correlation between the cyclic period (PCYC) and rotational period (PROT).

Our correlation between the rotational amplitude (AMP-R) and the cyclic amplitude (AMP-C) for all of the candidate stars combined reveals a moderately strong, positive correlation (fig. 13; $r=0.58$ and $p = 2.26e-8$). This strongly suggests that stars with higher rotational amplitudes tend to also exhibit higher cyclic amplitudes, reinforcing the idea that strong star spot activity at short-term rotational scales is often accompanied by significant long-term magnetic variability.

When cluster data are analysed separately, the correlation analysis between rotational amplitude (AMP-R) and cyclic amplitude (AMP-C) continue showing a moderately strong, positive correlation for both candidate stars coming from the M45 and Alpha Persei clusters, with Alpha Persei ones exhibiting a stronger correlation. In the case of M45 stars, the correlation coefficient ($r = 0.70$, $p = 0.00000272$), indicates that stars with higher short-term rotational amplitudes generally show larger long-term cyclic variations, although other factors

likely influence AMP-C as well. In contrast, Alpha Persei stars exhibit a slightly lower, but still moderately strong correlation ($r = 0.52$, $p = 0.00020$), that continues to be statistically significant. These differences are illustrated in fig. 11. The combined results of both datasets without any differentiation among the clusters are depicted in fig. 17.

Correlation between AMP-R and AMP-C for M45 and Alpha Persei Clusters

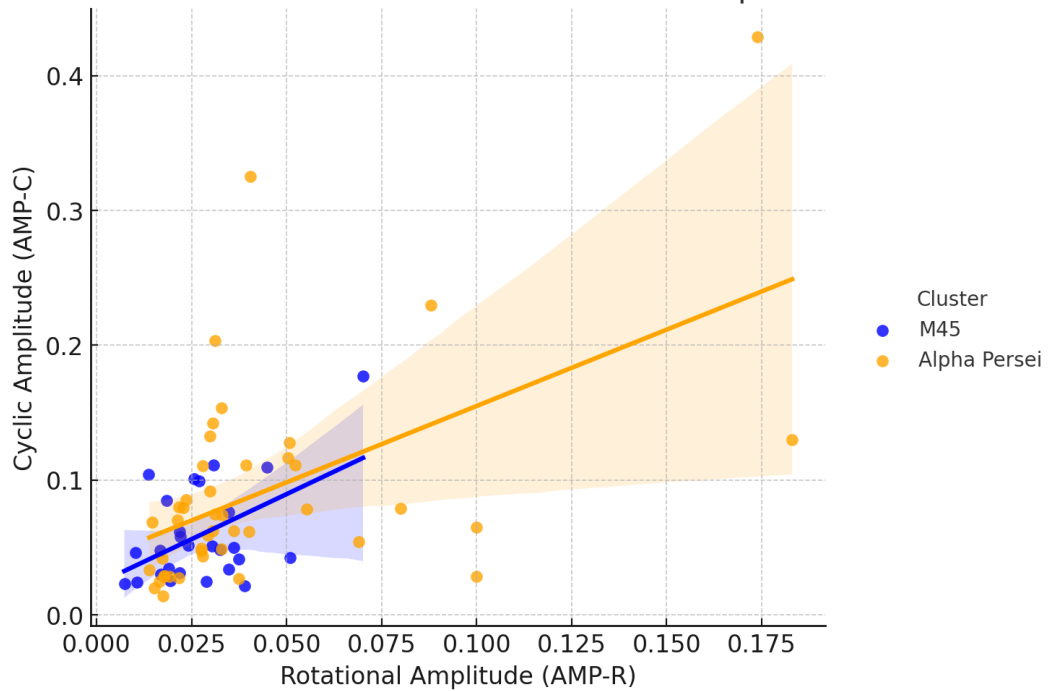


Figure 13: Correlation between Rotational Amplitude versus Cyclic Period Amplitude. Datasets from both clusters exhibit a moderately strong correlation.

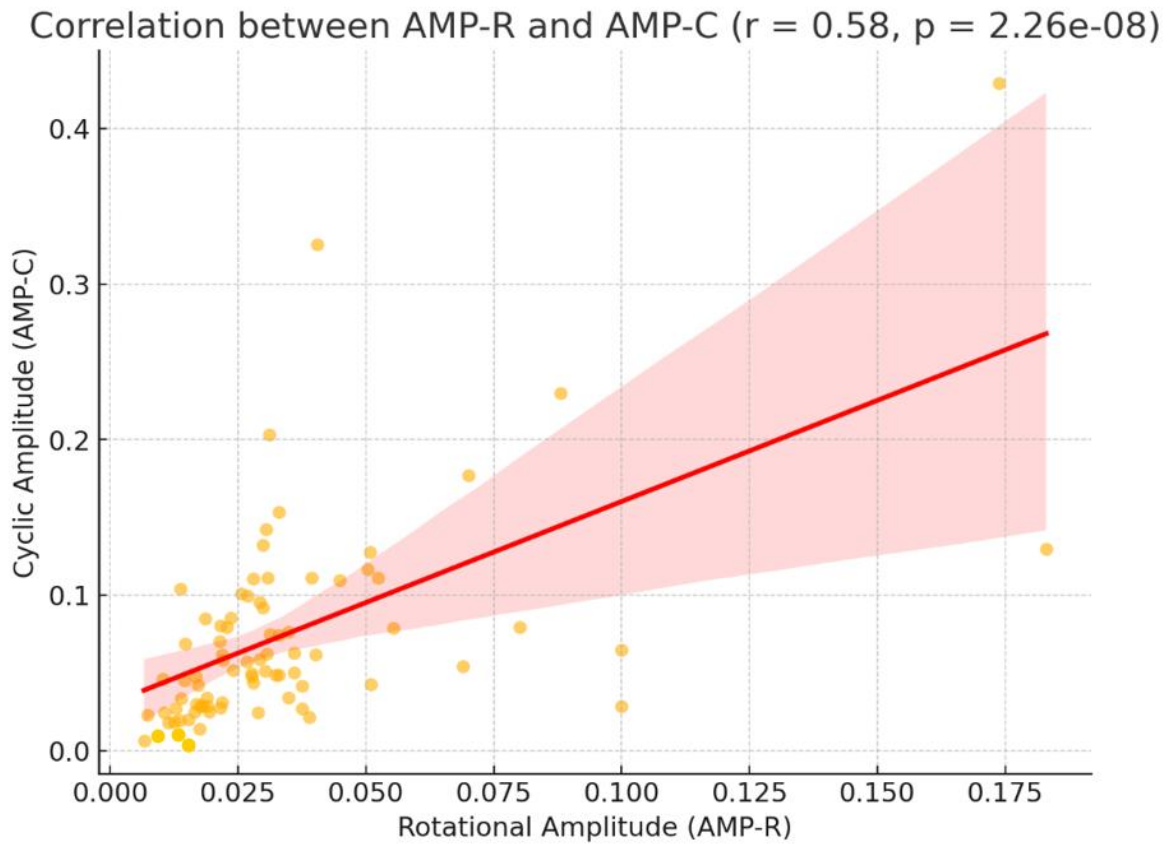


Figure 14: Combined datasets from Alpha Persei and M45 clusters showing a correlation between amplitude of the rotation period against the amplitude of the cycle period.

5 Conclusions

This study provides an insight into the mechanisms of BY Draconis stars after we have updated the cyclic periods (PCYC) of a set of chosen stars found within the M45 and Alpha Persei star clusters with previously unknown periodicity data in the VSX database. By then supplementing our processed observations collected by four astronomy observatories from the ASPIRE network (ASPIRE, 2024) with ASAS-SN data, we are able to confirm previously uncertain periods and established new periodicities for these chosen stars.

Following this processing and data analysis, we proceeded to provide valuable insights into these stars from two different clusters regarding the interplay between stellar rotation that is exhibited through amplitude variations over time, magnetic activity that is linked with the presence of star spots, and long-term cyclic variability that reflects on the magnetic cycle. While some expected relationships were observed, the findings highlight a complex scenario that is affected by the process of stellar evolution, binarity, and dynamo mechanisms.

We observed that the correlation between rotation period (PROT) and rotational amplitude (AMP-R) was generally weak across the candidate stars. This implies that while faster rotators tend to exhibit higher rotational amplitude, the large scatter in the data suggests that there are additional factors at play, such as star spot distribution, inclination effects, and binarity.

A combined, moderately positive correlation of $r = 0.35$ ($p = 0.00155$) was observed between the cyclic amplitude (AMP-C) and the cyclic period (PCYC), reinforcing the idea that stronger magnetic fields take longer to complete a full activity cycle. When cluster data was analyzed separately, this relationship was even stronger for our candidate stars in M45 ($r = 0.44$ and $p = 0.0215$) than with those in Alpha Persei ($r = 0.33$ and $p = 0.0285$), suggesting that older stars exhibit more developed and stable-structured long-term magnetic cycles. These findings agree with previous studies, confirming that highly active BY Draconis stars that exhibit pronounced variability tend to have longer magnetic cycles.

The strongest correlation found by this study was between rotational amplitude (AMP-R) and cyclic amplitude (AMP-C) indicating that stars with a more pronounced rotational amplitude, tend to exhibit distinct long-term cyclic variability (i.e. higher magnetic cycle amplitude). This trend was observed for the candidate stars found in both clusters, with M45 showing a stronger correlation ($r = 0.70$ and $p = 0.00000272$) than its cluster counterpart, Alpha Persei ($r = 0.52$ and $p = 0.00020$). This supports the idea that short-term rotational modulation (i.e. amplitude) is closely tied to the long-term stellar magnetic cycles, reinforcing the connection between rotation-driven activity and magnetic cycle strength.

An important aspect of this study concerned the examination of the relationship between rotation period (PROT) and cyclic period (PCYC). Across the whole dataset that encompass both clusters, the correlation was very weak and statistically not significant ($r = -0.03$ and $p = 0.815$). This suggests that the rotation period on its own does not strongly determine the duration of magnetic cycles. However, when individual cluster data were analyzed separately, M45 exhibited a weak negative correlation ($r = -0.36$ and $p = 0.0628$), implying that stars with longer rotation periods tend to have shorter cyclic periods, likely due to magnetic braking effects. In contrast, Alpha Persei showed a weak positive correlation ($r = 0.31$ and $p = 0.0428$), implying that in this younger stellar cluster, stars with longer rotation periods tend to have longer cyclic periods, reflecting an evolving relationship between rotation and magnetic activity.

Acknowledgements: This research has made use of the International Variable Star Index (VSX) database, operated by the American Association of Variable Star Observers (AAVSO), Cambridge, Massachusetts, USA. We acknowledge the AAVSO and its community of contributors for maintaining and curating this important dataset. The ongoing efforts of the AAVSO to provide such essential resources to the continued development of variable star research is acknowledged.

References

Alekseev, I.Y. 1999, *Bull. Crime. Astrophys. Obs.*, 95, 69

- ASPIRE 2024, Asteroid and Stellar Photometric Research Group, <https://www.aspireastro.net>
- Balona, L.A. 2020, arXiv e-prints, <https://arxiv.org/abs/2008.06305>
- Bellm, E. 2014, in The Third Hot-wiring the Transient Universe Workshop, Vol. 27, <https://arxiv.org/abs/1410.8185>
- Bopp, B.W., & Fekel, F. Jr. 1977, AJ, 82, 490
- Boyle, A.W., & Bouma, L.G. 2023, AJ, 166, 14
- Brown, A.G.A., Vallenari, A., Prusti, T., et al. 2018, A&A, 616, A1
- Chahal, D., de Grijs, R., Kamath, D., & Chen, X. 2022, MNRAS, 514, 4932
- Charbonneau, P. 2010, Living Rev. Sol. Phys., 7, 3, <https://doi.org/10.12942/lrsp-2010-3>
- Chen, X., Wang, S., Deng, L., et al. 2020, ApJS, 249, 18
- Cutri, R.M., Skrutskie, M.F., Van Dyk, S., et al. 2003, VizieR Online Data Catalog, II/246
- de Grijs, R., & Kamath, D. 2021, Universe, 7, 440, <https://doi.org/10.3390/universe7110440>
- Gaia Collaboration 2020, VizieR Online Data Catalog, I/350
- Hall, D.S. 1991, in IAU Colloq. 130, The Sun and Cool Stars: Activity, Magnetism, Dynamos, ed. I. Tuominen, D. Moss, & G. Rüdiger (Berlin: Springer), 353
- Henden, A.A., Templeton, M., Terrell, D., et al. 2016, VizieR Online Data Catalog, II/336
- Jeffers, S.V., Kiefer, R., & Metcalfe, T.S. 2023, Space Sci. Rev., 219, 54
- Kochanek, C.S., Shappee, B.J., Stanek, K.Z., et al. 2017, PASP, 129, 104502
- Lanzafame, A.C., Distefano, E., Messina, S., et al. 2018, A&A, 616, A16
- Mamajek, E. 2019, A Modern Mean Dwarf Stellar Color and Effective Temperature Sequence, http://www.pas.rochester.edu/~emamajek/EEM_dwarf_UBVIJHK_colors_Teff.txt
- Neff, J.E., Walter, F.M., Rodonò, M., & Linsky, J.L. 1989, A&A, 215, 79
- Nielsen, M.B., Gizon, L., Cameron, R.H., & Miesch, M. 2019, A&A, 622, A85
- Oláh, K., Seli, B., Kővári, Z., Kriskovics, L., & Vida, K. 2022, A&A, 668, A101
- Paegert, M., Stassun, K.G., Collins, K.A., et al. 2021, VizieR Online Data Catalog, IV/39
- Paunzen, E., & Vanmunster, T. 2016, Astron. Nachr., 337, 239
- Radick, R.R., Thompson, D.T., Lockwood, G.W., Duncan, D.K., & Baggett, W.E. 1987, ApJ, 321, 459
- Rybizki, J., Demleitner, M., Bailer-Jones, C., et al. 2020, PASP, 132, 074501
- Sanghi, A., Vanderbosch, Z.P., & Montgomery, M.H. 2021, AJ, 162, 133
- Scargle, J.D. 1982, ApJ, 263, 835
- Schlafly, E.F., & Finkbeiner, D.P. 2011, ApJ, 737, 103
- Schrijver, C.J., & Zwaan, C. 2008, Solar and Stellar Magnetic Activity (Cambridge: Cambridge Univ. Press)
- Scholz, A., & Eislöffel, J. 2007, MNRAS, 381, 1638
- Soriano, M.F., & Strassmeier, K.G. 2017, A&A, 597, A101
- Shappee, B.J., Prieto, J.L., Grupe, D., et al. 2014, ApJ, 788, 48
- Tonry, J.L., Denneau, L., Flewelling, H., et al. 2021, VizieR Online Data Catalog, J/ApJ/883/102
- Tout, C.A., & Pringle, J.E. 1992, MNRAS, 256, 269
- VanderPlas, J.T. 2018, ApJS, 236, 16
- Vida, K., Oláh, K., Kővári, Z., et al. 2009, A&A, 504, 1021
- Watson, C.L., Henden, A.A., & Price, A. 2006, in SAS Symp., Vol. 25, 47
- Zechmeister, M., & Kürster, M. 2009, A&A, 496, 577